A Two Step Spatio-Temporal Filtering Scheme for Smart Antennas Compared to a Multi-User Maximum Likelihood Algorithm

Christopher Brunner,[1,2] *Martin Haardt,*[1] *Christof Farsakh,*[2,†] *and Josef A. Nossek*[2]

1. Siemens AG, Mobile Networks, OEN MN P 36
Hofmannstr. 51, D-81359 Munich, Germany
Phone: +49 (89) 722-29480, Fax: +49 (89) 722-44958
E-mail: Martin.Haardt@oen.siemens.de

2. Institute of Network Theory and Circuit Design
Munich University of Technology, D-80290 Munich, Germany
Phone: +49 (89) 289-28511, Fax: +49 (89) 289-28504
E-Mail: chbr@nws.e-technik.tu-muenchen.de

Abstract — **Future wireless communication systems require an increased spectral efficiency to accommodate the growing number of users and permit connections with higher data rates. To this end, smart antenna arrays utilizing adaptive beamforming techniques on the uplink as well as the downlink enable space division multiple access (SDMA). Furthermore, the range is increased significantly which is of great advantage in rural areas. We present an algorithm in which a two-dimensional (2-D) spatial filtering scheme based on 2-D Unitary ESPRIT is used to separate the dominant wavefronts. Then the separated wavefronts are assigned to the users by correlating them with known training sequences. To obtain temporal equalization, all wavefronts assigned to a particular user are passed on to the different diversity branches of a (single-user) Viterbi equalizer. The performance of this two step spatio-temporal filter is compared to a computationally more expensive algorithm in which a joint multi-user maximum likelihood equalizer is applied to the impulse responses of all co-channel users. The impulse responses are estimated by exploiting the training sequences. Monte Carlo simulations for synthetic and realistic scenarios allow a performance evaluation of both schemes based on the uplink bit error ratio. Note that (both) data detection schemes require spatially well separated users to obtain good performance. Therefore, an intelligent channel assignment strategy is examined in connection with both schemes.**

1. Introduction

In future F/TDMA wireless communication systems, SDMA enables mobiles that are located at spatially distinct angles from the base station to operate on the same frequency as well as in the same time slot [12]. In [6, 5], we have considered the performance of a GSM system enhanced by a 2-D spatial filter based on 2-D Unitary ESPRIT in terms of the signal to interference plus noise ratio. Here, we extend the spatial filter of [6] to provide temporal equalization and (single-user) maximum likelihood sequence estimation (MLSE) for all wavefronts assigned to the same user. The MLSE equalizer is efficiently implemented with a Viterbi-like algorithm [2, 9]. This allows a performance evaluation based on the bit error ratio (BER). The BERs are determined for a joint multi-user maximum likelihood algorithm (MU-ML) as well [2, 3], thus allowing a comparison between both schemes. To ensure realistic scenarios, propagation data of the downtown of Munich is generated by a sophisticated ray tracing tool developed at the University of Karlsruhe [1].

This paper is organized as follows. The 2-D data model is introduced in Section 2. Section 3 and Section 4 explain the spatio-temporal filter (STF) and the MU-ML scheme, respectively. In Section 5, simulation results of synthetic and realistic scenarios compare the performance of both schemes. Spatial separation of mobiles may be achieved by intelligent channel assignment strategies that are based on the directions of arrival (DOA). Here, we consider the channel assignment strategy suggested in [3] for both schemes. Conclusions are drawn in Section 6.

†C. Farsakh is now with Ericsson Eurolab Deutschland GmbH, Äußere Bayreuther Str. 350, D-90411 Nürnberg, Germany, Phone: +49 (911) 5127 537, E-Mail: Christof.Farsakh@eedn.ericsson.se.

2. 2-D Data Model

Without loss of generality, we restrict our discussion to uniform rectangular arrays (URAs) consisting of $M = M_x \times M_y$ antennas lying on a rectangular grid in the x-y plane. The inter-element spacing in x- and y-direction will be called Δ_x and Δ_y, respectively. Incident on a URA of M antennas are d narrowband planar wavefronts with wavelength λ, azimuth ϕ_i, and elevation θ_i, $1 \leq i \leq d$. Assume that the emitting sources are narrowband and in the far field such that the d wavefronts impinging on the array are planar. The narrowband assumption is, for instance, valid for the current GSM system [13]. Recall that these d wavefronts are due to actual sources as well as scatterers (coherent multipath). Let $u_i = \cos\phi_i \sin\theta_i$ and $v_i = \sin\phi_i \sin\theta_i$, $1 \leq i \leq d$,

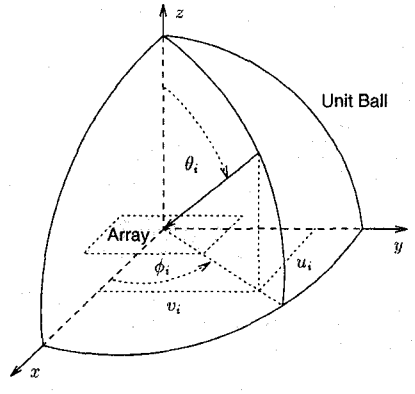

Figure 1: Definitions of azimuth ($-180° < \phi_i \leq 180°$) and elevation ($0° \leq \theta_i \leq 90°$). The direction cosines u_i and v_i are the rectangular coordinates of the projection of the corresponding point on the unit ball onto the equatorial plane (u-v plane).

denote the direction cosines of the ith source relative to the x- and y-axes as illustrated in Figure 1.

The complex envelopes of the d impinging wavefronts at a reference antenna are combined to the column vector $s(t_n) \in \mathbb{C}^d$. Let X denote an $M \times N$ complex data matrix composed of N samples $x(t_n), 1 \leq n \leq N$, where

$$\begin{aligned} X &= \left[\, x(t_1) \quad x(t_2) \quad \cdots \quad x(t_N) \,\right] \\ &= A \left[\, s(t_1) \quad s(t_2) \quad \cdots \quad s(t_N) \,\right] + N \\ &= A \cdot S + N. \end{aligned} \tag{1}$$

Here, the matrix N contains the (colored) noise samples. The array steering matrix

$$A = \left[\, a(\mu_1, \nu_1) \quad a(\mu_2, \nu_2) \quad \cdots \quad a(\mu_d, \nu_d) \,\right] \tag{2}$$

contains the 2-D steering vectors $a(\mu_i, \nu_i)$, $1 \leq i \leq d$, of the d impinging wavefronts, where the spatial frequencies μ_i and ν_i are scaled versions of the corresponding direction cosines, namely $\mu_i = \frac{2\pi}{\lambda}\Delta_x u_i$ and $\nu_i = \frac{2\pi}{\lambda}\Delta_y v_i$.

3. Two Step Spatio-Temporal Filter

3.1. 2-D Spatial Filter

The directional channel parameters such as azimuth and elevation of the $d' \leq d$ dominant wavefronts are estimated based on the knowlegde of the array. 2-D Unitary ESPRIT represents an efficient way to estimate the spatial frequencies μ_i and ν_i from the noise-corrupted data matrix $\boldsymbol{X}$ in (1) and automatically achieves their correct pairing [5]. Notice that the M antennas are not required to be omnidirectional as long as all of them have identical (possibly angle dependent) characteristics.

Wavefronts of very similar delay originating from the same source are highly correlated or even coherent due to multipath propagation. However, more than two equally delayed wavefronts do not occur in most multipath scenarios. 2-D Unitary ESPRIT inherently includes forward-backward averaging, i.e., is applicable if no more than two highly correlated wavefronts impinge at the array [5].[1] The 2-D steering vectors $\boldsymbol{a}(\mu_i, \nu_i)$ and an appropriate array steering matrix $\boldsymbol{A}$ are constructed based on the estimated spatial frequency pairs $[\mu_i, \nu_i]$, $1 \leq i \leq d'$, cf. (2). Then we calculate the linear minimum variance unbiased estimate of $\boldsymbol{S}$ by choosing the weighted least squares or Gauss-Markov estimate

$$\begin{aligned} \boldsymbol{W} &= \left(\boldsymbol{A}^H \boldsymbol{R}_{nn}^{-1} \boldsymbol{A}\right)^{-1} \boldsymbol{A}^H \cdot \boldsymbol{R}_{nn}^{-1} \\ \boldsymbol{S} &= \boldsymbol{W} \cdot \boldsymbol{X} \in \mathbb{C}^{d' \times N}, \end{aligned} \tag{3}$$

where $\boldsymbol{R}_{nn}$ denotes the estimated noise covariance matrix. Unitary ESPRIT is easily adapted to take colored noise into account as explained in [7].

3.2. Temporal Equalization

Once the dominant wavefronts have been separated with respect to their distinct 2-D arrival angles, the correlation coefficients between vectors containing time-shifted versions of the transmitted training sequences and vectors containing the temporal samples of the estimated wavefronts (at the output of the 2-D spatial filter) are calculated.

To determine the corresponding timing offsets, several versions of each training sequence are used. The sampling points of subsequent versions of the same training sequence are delayed by T_b/V with respect to one another ($V = 16$ was used in the simulations), where T_b denotes the bit duration.[2] Thus, the correlation coefficients depend on the user, on the wavefront, and on the delay. The magnitude of these correlation coefficients is employed to associate the estimated wavefronts with the users. Hereby, each user is associated with at least one wavefront by choosing the wavefront with the largest correlation coefficient for the corresponding user as explained in [6]. Further wavefronts are assigned according to the comparison of the magnitude of their correlation coefficients.

Notice that the separated wavefronts are influenced by noise and interference. If noise and interference arrive approximately uniformly from all directions, the power of this influence, e.g., the noise amplification, depends only on the corresponding beam pattern. In most cases, the correlation between these disturbances is small. Therefore, the performance of the equalizer is improved if the noise amplification of all wavefronts assigned to a user is equal. Recall that each beam pattern is determined by the corresponding row $\boldsymbol{w}_i^H$ of $\boldsymbol{W}$ in (3). Hence, the power of the noise (and interference) amplification of the ith wavefront equals $\boldsymbol{w}_i^H \cdot \boldsymbol{w}_i$. To achieve equal noise amplification, the wavefronts are, therefore, weighted according to

$$\boldsymbol{S}' = \left(\mathrm{diag}\{\sqrt{\boldsymbol{w}_i^H \cdot \boldsymbol{w}_i}\}_{i=1}^{d'}\right)^{-1} \cdot \widehat{\boldsymbol{S}}, \quad \text{where} \quad \boldsymbol{W} = \begin{bmatrix} \boldsymbol{w}_1^H \\ \boldsymbol{w}_2^H \\ \vdots \\ \boldsymbol{w}_{d'}^H \end{bmatrix}.$$

Next the wavefronts (per user) are fed into several diversity branches of the subsequent temporal equalizer where they are applied to a Viterbi-like algorithm [2, 9].

4. Multi-User Maximum-Likelihood Algorithm

Let us give a brief overview of the MU-ML scheme. The envelopes of the signals of the K users are denoted as $u_k(t)$. Sampling the envelopes $u_k(t)$ at the symbol rate $1/T$ over the duration of one GSM burst yields the complex valued sequences $u_{k,l}$, $1 \leq l \leq L$. The GSM burst is sampled L times. Considering a limited channel memory C, the time delays τ of the multipath signals are approximated by discrete delays $\tau_{\min} + (c-1)T$, $1 \leq c \leq C$. The signal originating from user k and received at antenna m may then be expressed as

$$x_{m,l} = \sum_{k=1}^{K} \sum_{c=1}^{C} h_{k,m,c} u_{k,l+1-c} \quad \forall \quad 1 \leq l \leq L, \tag{4}$$

where $\boldsymbol{h}_{k,m}^T = [h_{k,m,1} \ldots h_{k,m,C}]$ denotes the sampled channel impulse response corresponding to the channel between the user k and the antenna m. With (4), the impulse responses of all co-channel users at all antennas are estimated by exploiting the training sequences [2] which are part of $u_{k,l}$. With the knowledge of the data matrix $\boldsymbol{X}$ and the estimated impulse responses $\boldsymbol{h}_{k,m}^T$, temporal equalization and multi-user MLSE estimation are performed, which may be implemented with a Viterbi-like algorithm [2, 9].

A significant part of the computational complexity is caused by equalization which is similar for both schemes if only one user accomodates an F/TDMA slot. Since the MU-ML scheme equalizes all users jointly, the computational complexity increases exponentially with each user [2]

$$N_{\min} = M(K_j C + 1) 2^{(K_j C + 1)}.$$

Here, $N_{\min}$ denotes the minimum number of floating point operations and K_j denotes the number of users which are equalized jointly. The GSM system was designed for propagation conditions which require $C = 5$. Therefore, more than two users cannot be equalized jointly due to hardware limits ($K_j = K$). For comparison, the computational complexity of the STF ($K_j = 1$) increases only linearly with the number of users K.

5. Simulation Results

To illustrate and explain the differences in performance due to the different underlying models of both schemes, we begin with simulation results for a scenario in which one wavefront is assigned to one user and, therefore, no angular spread and no fading occur. Next we choose more complex scenarios until we arrive at realistic scenarios in which many wavefronts with different delays are assigned to several co-channel users, thus producing (fast) fading effects, interference, and angular spread. Finally the channel assignment strategy is examined for both schemes [3].

The simulation results to follow were realized at the link level. We look at one cell only and emulate neighboring cells by adding additive

[1] More than two highly correlated wavefronts (per user) could be decorrelated by using spatial smoothing [5] as a preprocessing step at the cost of a reduced antenna aperture, i.e., more samples would be necessary to reach the same estimation accuracy. Furthermore, the maximum number of wavefronts which can be estimated is reduced. Note that spatial smoothing is not used in the simulations presented in Section 5.

[2] This provides an efficient alternative to correlation based synchronization techniques that require oversampling of the received signals as, for instance, discussed in [4]. Here, we only sample once per symbol.

white Gaussian noise. A 4×4 URA was used in all scenarios if not stated otherwise. We have taken one snapshot per bit, yielding a total of 148 snapshots per burst. The other simulation parameters were chosen in accordance with the current GSM standard, e.g., GMSK modulated bursts of 148 bits including a midamble (training sequence) of 26 bits were transmitted. The total power of each user is normalized to one. The signal to noise ratio (SNR) is defined as the ratio between the total power of a user which equals one and the power of the additive white noise. Fast fading is generated for the angular spread scenario and the realistic scenarios below by multiplying the wavefronts of each burst with random phase shifts. These phase shifts differ for each simulated burst.

5.1. Synthetic Scenarios

The first scenario consists of a single wavefront which arrives at the URA with an azimuth and elevation of $(15°, -15°)$, respectively. With only one antenna, the MU-ML scheme corresponds to the data detection scheme of a conventional GSM system. In Figure 2, the (right) dashed curve denotes the BER as a function of the SNR without coding and interleaving averaged over 1000 trial runs. The maximum antenna gain is determined by

$$G(M) = 10 \cdot \log_{10} M.$$

With 16 antennas instead of one, $G(16) = 12.04$ dB holds. This gain is obtained by the STF, cf. Figure 2. The solid curve denotes the BER as a function of the SNR without coding and interleaving averaged over 1000 trial runs. The DOAs were estimated with samples from 8 bursts which corresponds to one trial run. Thus, the range is increased significantly which is of great advantage in rural areas. Now we extend the first scenario by adding two well separated users each characterized by one wavefront. The impinging wavefronts have arrival angles of $(15°, -15°)$, $(45°, 0°)$, and $(75°, -15°)$. The STF is able to separate all three wavefronts perfectly. The solid curve which denotes the BER as a function of the SNR is identical with the curve corresponding to the previous scenario with only one wavefront. The adjacent dashed curve denotes the BERs of the three wavefronts separated by the MU-ML scheme. The MU-ML scheme performs worse than the STF for the following reasons:

- The STF reduces the influence of the noise to a higher degree since only the DOAs of interest are amplified.
- The STF uses all samples for parameter estimation and is not restricted to the training sequence which comprises only 16% of a GSM burst.
- The training sequences themselves are not completely orthogonal.[3]

In realistic scenarios, each user is characterized by more than one wavefront due to scattering, diffraction, reflection, etc. Therefore, the influence of angular spread on both schemes is examined in the following scenario. Two-dimensional angular spread is generated by DOAs of 100 impinging wavefronts of equal power (of one user) which are spread uniformly over an azimuth and an elevation sector.[4] The SNR equals 0 dB. Again, the dominant DOAs were estimated with samples from 8 bursts. Note that the STF estimates only the dominant wavefronts in a realistic scenario with a large number of wavefronts. The number of dominant wavefronts d' must be estimated from the available measurements. A variety of detection schemes has been proposed in the literature. The well-known minimum description length (MDL) criterion [14, 15] overestimates especially for high signal to

[3] Whereas the autocorrelation properties of the training sequences are optimized for equalization in a conventional GSM system, the crosscorrelation properties become more important for separation. Therefore, we used modified training sequences in our simulations.

[4] We define angular spread as the distance from the leftmost possible angle to the rightmost possible angle of each sector.

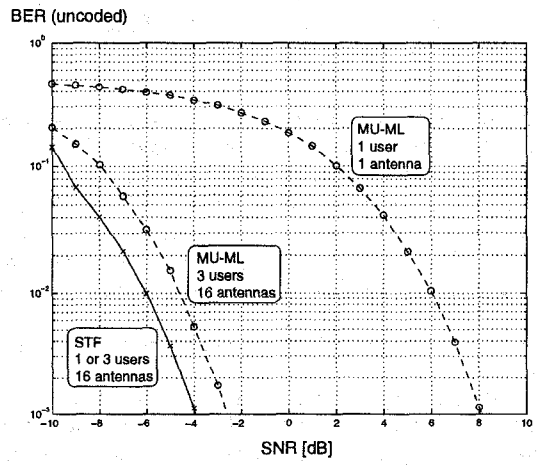

Figure 2: With $M = 4 \times 4$ antennas, the STF obtains an antenna gain of $G(16) = 12.04$ dB.

noise ratios. Therefore, we chose a threshold criterion [11]. For a 2-D angular spread of 20°, for instance, the estimated number of dominant wavefronts varies between one and two. Figure 3 shows the BER as a function of the 2-D angular spread averaged over 100 trial runs. Due to the underlying model which assumes discrete DOAs, the STF handles small angular spread well. The MU-ML scheme, however, exploits the spatial diversity to a higher degree and copes better with a 2-D angular spread above 10°.

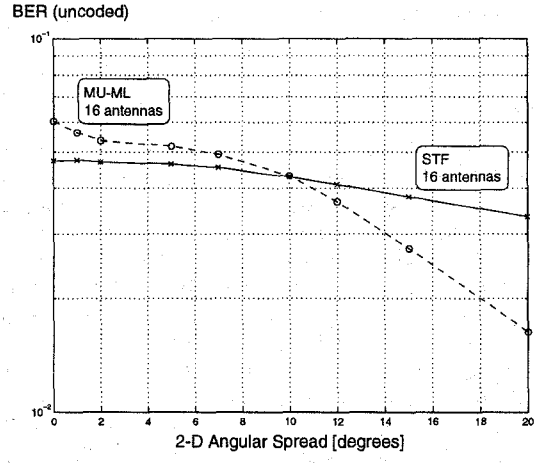

Figure 3: Due to the underlying model, the STF handles small angular spreads well.

5.2. Realistic Scenarios

The next scenario is based on a three-dimensional topographical model of downtown Munich, where the height of the base station is 26 meters and the height of the transmitter at the mobiles is 2 meters, cf. Figure 4. In this urban environment, the propagation conditions at $f_c = 1$ GHz are predicted via 3-D ray tracing by taking into account wave interactions like diffraction and scattering over each propagation path [10]. Ray tracing algorithms developed at the University of Karlsruhe yield the channel impulse response of each propagation path in terms of its attenuation, time delay, 2-D launching angle (at the transmitter), and 2-D arrival angle (at the receiver). The resulting coverage predictions are in a close agreement with measurements taken in the same urban area [1]. The 3-D plots in Figure 5 show the power of the impinging wavefronts as a function of the direction cosines in the u-v plane for users in three different positions, cf. Figure 4. Although the 2-D arrival angles occur in fairly large clusters, the principal portion of the received energy is concentrated in fairly small areas in the u-v plane.

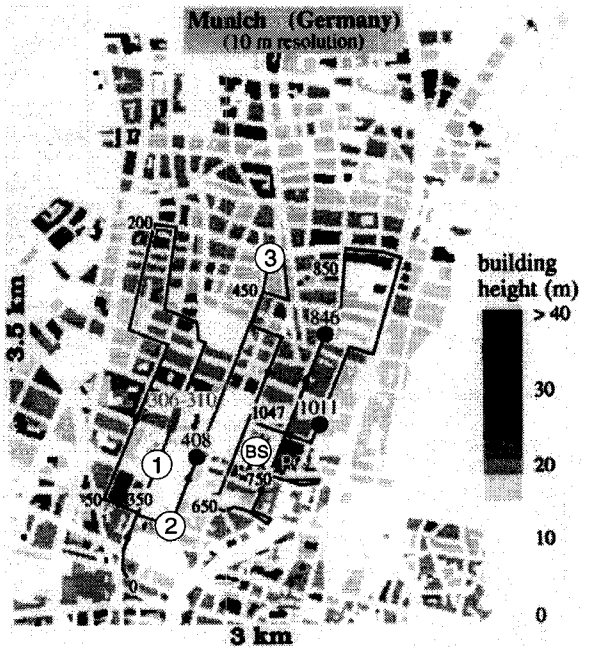

Figure 4: Map of downtown Munich showing the location of the base station (BS) and of the three users.

Now we apply this scenario to both schemes. The STF estimated the dominant DOAs using samples from 32 bursts which corresponds to one trial run. The 2-D arrival angles (predicted via ray tracing) are assumed to be stationary over this interval. To mitigate the influence of (fast) fading, interference, etc., the signals were coded and interleaved. If the model order, e.g., the number of dominant wavefronts is increased, the number of samples used for parameter estimation must increase as well to maintain the same DOA estimation accuracy. This is not reflected properly by the threshold criterion [11]. A good performance was obtained by setting the model order to 4 which corresponds to the visual impression of the users plotted in Figure 5.[5] Figure 5 plots the BERs of the three users as a function of the SNR averaged over 300 trial runs for both schemes. For three users, the STF is computationally far less complex. Moreover, the STF also performs significantly better than the MU-ML scheme for low SNRs. Notice that the spatial filter in (3) generates beam patterns which put "zeros" in the $d' - 1$ dominant DOAs of interferers and "ones" in the dominant DOA of interest. Since all users in realistic scenarios have an angular spread, cf. Figure 5, the spatial filter is not able to suppress interfering users completely. Accordingly, user 2 is limited more by interference than by noise for high SNRs, especially since this user fades strongly and the STF does not equalize jointly. The MU-ML scheme benefits from joint equalization and is, therefore, less sensitive to fading.

A DOA sensitive channel allocation scheme can assign spatially badly separable users to different channels as explained in [3]. With K users operating in the same F/TDMA channel, the beampatterns to separate the users $k = 1 \ldots K$ from each other (on the downlink) must be produced by the weights $w_1 \ldots w_K$. The corresponding beamforming problem may be expressed as

$$\underset{w_1 \ldots w_K}{\text{minimize}} \left\{ P = \sum_{k=1}^{K} w_k^H w_k \right\} \qquad (5)$$

with the constraints for $k = 1 \ldots K$ according to

$$\frac{w_k^H C_k w_k}{\text{SINR}} = N_k + \sum_{\substack{l=1 \\ l \neq k}}^{K} w_l^H C_k w_l, \quad \text{where} \quad C_k = \sum_{q=1}^{d_k} A_{kq}^2 a_{kq} a_{kq}^H.$$

The medium term channel of each user $k = 1 \ldots K$ can be efficiently described by means of the $M \times M$ spatial covariance matrix C_k. Moreover, d_k denotes the number of wavefronts of user k, and A_{kq} and a_{kq} are the amplitude and the steering vector of user k and wavefront $q = 1 \ldots d_q$, respectively. The power of K users which is required to achieve a fixed SINR is denoted by $P_{\min}$ in case of K users broadcasting in K different F/TDMA channels and is denoted by P in case of K users broadcasting in one F/TDMA channel. The ratio $P/P_{\min}$ may then be used as a measure for spatial separability.

In the next simulation two positions, e.g., their propagation data generated by the raytracing model, are selected randomly. We chose SINR = 20 dB to take into account fast fading. If $P/P_{\min} < 0.1$ dB holds, both data detection schemes are applied. The STF estimates the dominant DOAs using samples from 32 bursts. The BERs plotted over the SNR in Figure 6 are averaged over 300 scenarios and over both users. Notice that the parameters chosen for the channel selection scheme avoid scenarios in which incorrect detection is caused by interference ($P/P_{\min} < 0.1$ dB) in combination with fast fading (SINR = 20 dB). Hence, the performance of both data detection schemes is similar, cf. Figure 6.

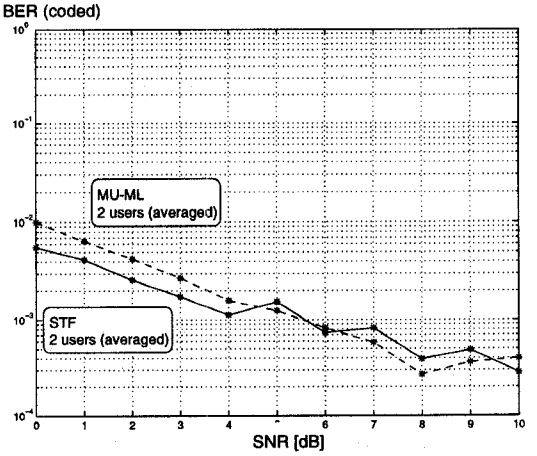

Figure 6: The dashed and the solid line denote the BER averaged over 300 scenarios and over two users for the STF and the MU-ML scheme, respectively.

6. Concluding Remarks

Clearly, the use of an adaptive antenna array at the base station achieves a significant improvement of the BER over a wide range of SNRs. Thereby, the received interference is reduced and the range of a base station is increased significantly.

The main advantage of the STF is that the computational complexity increases only linearly with each user and not exponentially due to joint equalization. To avoid the computational complexity of the MU-ML scheme and to handle degradation due to interference and fading, the STF could (iteratively) subtract the user received best (according to the correlation coefficients) from the remaining users. Moreover, the beamforming algorithm should take into account angular spread. This would also ease the requirements on DOA accuracy and, therefore, on the model order estimation algorithm. A further increase in performance may be obtained by exchanging the Viterbi-like algorithm used for equalization by a SOVA (Soft Output Viterbi Algorithm) equalizer [8].

[5] In general, the number of samples is limited by the instationarity of users and interferers which may lead to an interesting tradeoff. If the model order increases, spatial diversity may be exploited to a higher degree at the cost of reduced accuracy. Reduced accuracy translates into separated wavefronts with more noise and higher interference.

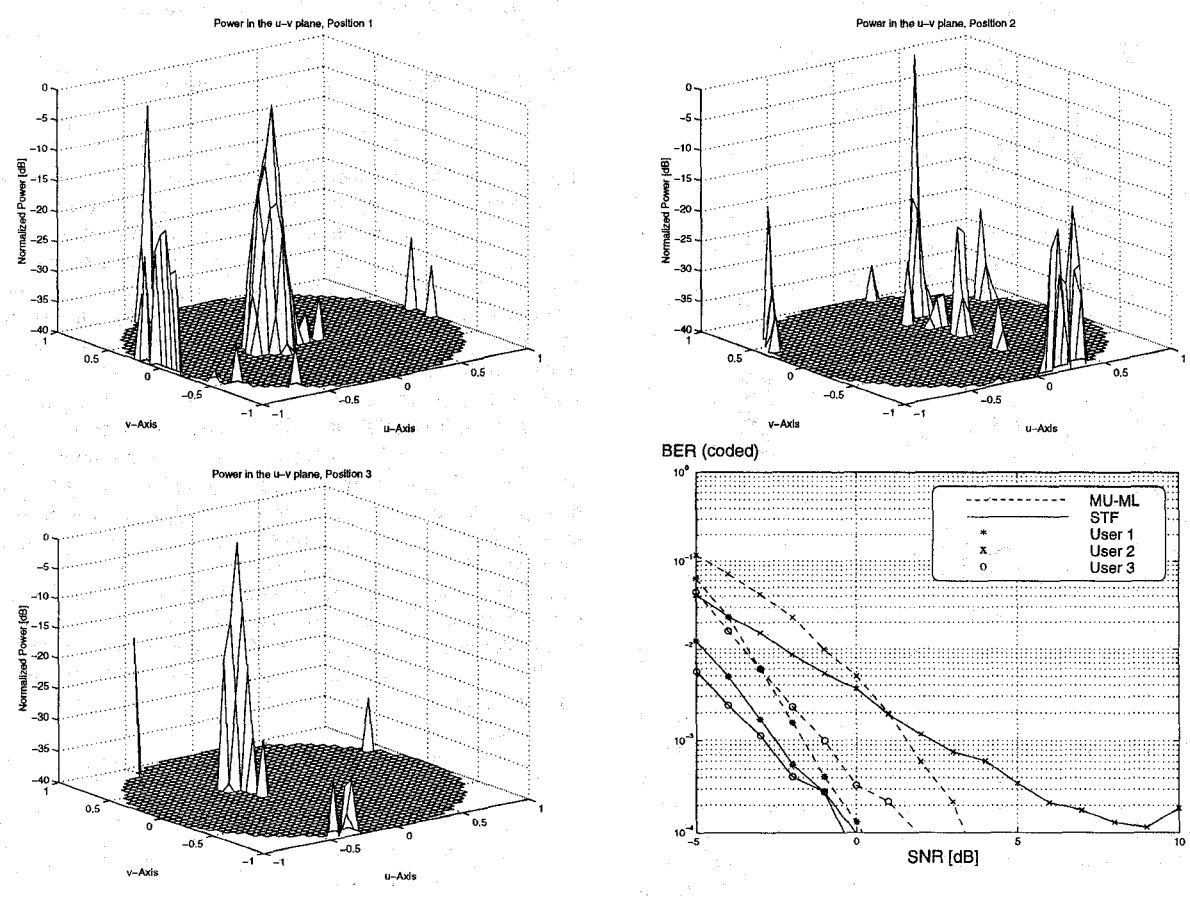

Figure 5: Distribution of the 2-D arrival angles of users 1, 2, and 3 in the u-v plane: The 3-D plots show the power of the impinging wavefronts as a function of the direction cosines. The users are characterized by 313, 265, and 119 wavefronts, respectively. Bottom right: Comparison between both data detection schemes for these users.

Note that the channel parameters such as arrival angles, delays, and amplitudes estimated in the uplink may be exploited for the downlink as well. Employing, for instance, the estimated 2-D arrival angles for efficient downlink beamforming drastically reduces the interference generated by the base station towards adjacent cells as well.

Acknowledgment

The authors would like to thank Karlheinz Pensel for many productive discussions.

References

[1] D. J. Cichon, *Strahlenoptische Modellierung der Wellenausbreitung in urbanen Mikro- und Pikofunkzellen*, Ph. D. dissertation, University of Karlsruhe, Karlsruhe, Germany, Dec. 1994, in German.

[2] C. Farsakh, *SDMA - Raummultiplex in zellularen Mobilfunksystemen*, Ph. D. dissertation, Technical University of Munich, Institute of Network Theory and Circuit Design, Munich, Germany, Oct. 1997, in German.

[3] C. Farsakh and J. A. Nossek, "Data detection and channel allocation on the uplink of an SDMA mobile radio system", in *Proc. IEEE / IEE Int. Conf. on Telecommunications*, W. L. Lavery, Ed., vol. 3, pp. 813–818, Melbourne, Australia, Apr. 1997.

[4] J. Fuhl and E. Bonek, "Optimum antenna topologies and adaptation strategies for SDMA", in *Proc. IEEE GLOBECOM*, London, U. K., Nov. 1996.

[5] M. Haardt, *Efficient One-, Two-, and Multidimensional High-Resolution Array Signal Processing*, Shaker Verlag, Aachen, Germany, 1996, ISBN 3-8265-2220-6.

[6] M. Haardt, C. Brunner, and J. A. Nossek, "2-D Unitary ESPRIT for smart antenna arrays in mobile communications", in *Proc. IEEE / IEE Int. Conf. on Telecommunications*, W. L. Lavery, Ed., vol. 2, pp. 587–592, Melbourne, Australia, Apr. 1997.

[7] M. Haardt, C. Brunner, and J. A. Nossek, "Efficient high-resolution 3-D channel sounding", in *Proc. 48th IEEE Vehicular Technology Conf. (VTC '98)*, Ottawa, Canada, May 1998.

[8] J. Hagenauer and P. Höher, "A Viterbi algorithm with soft decision outputs and applications", in *Proc. IEEE GLOBECOM*, pp. 47.1.1–47.1.7, Dallas, USA, Apr. 1989.

[9] P. Jung, M. Naßhan, and Y. Ma, "Comparison of optimum detectors for coherent receiver antenna diversity in GSMtype mobile radio systems", in *Proc. 4th IEEE Int. Symp. on Personal, Indoor and Mobile Radio Commun. (PIMRC)*, pp. 54–58, Yokohama, Japan, Sept. 1993.

[10] T. Kürner, D. C. Cichon, and W. Wiesbeck, "Concepts and results for 3D digital terrain-based wave propagation models: An overview", *IEEE Journal on Selected Areas in Communications*, vol. 11, pp. 1002–1012, Sept. 1993.

[11] U. Martin, "Modeling the mobile radio channel by echo estimation", *Frequenz*, vol. 48, pp. 198–212, 1994.

[12] R. Rheinschmitt and M. Tangemann, "Performance of sectorised spatial multiplex systems", in *Proc. IEEE Vehicular Techn. Conf.*, vol. 1, pp. 426–430, Atlanta, GA, Apr. 1996.

[13] F. Vanpoucke, *Algorithms and Architectures for Adaptive Array Signal Processing*, Ph. D. dissertation, Katholieke Universiteit Leuven, Leuven, Belgium, Feb. 1995.

[14] M. Wax and T. Kailath, "Detection of signals by information theoretic criteria", *IEEE Trans. Acoustics, Speech, and Signal Processing*, vol. ASSP-33, pp. 387–392, Apr. 1985.

[15] G. Xu, R. H. Roy, and T. Kailath, "Detection of number of sources via exploitation of centro-symmetry property", *IEEE Trans. Signal Processing*, vol. 42, pp. 102–112, Jan. 1994.